Selective Electroless Nickel Plating of Particle Arrays on Polyelectrolyte Multilayers

Ilsoon Lee*

Department of Chemical Engineering and Materials Science, Michigan State University, East Lansing, Michigan 48824

Paula T. Hammond† and Michael F. Rubner‡

Department of Chemical Engineering and Department of Materials Science and Engineering, Massachusetts Institute of Technology, Cambridge, Massachusetts 02139

Received June 30, 2003. Revised Manuscript Received September 25, 2003

Selective electroless nickel plating was demonstrated at the micron scale on 3-D surface microstructures using a two-step method. The 3-D patterned and functional surface microstructures consisted of microparticles, polyelectrolyte multilayers, and self-assembled monolayers, which were built by microcontact printing and directed self-assemblies of polyelectrolytes and particles. Selectively nickel-plated surfaces were characterized with optical microscopy, X-ray photoelectron spectroscopy, scanning electron microscopy, and energy-dispersive X-ray spectroscopy. Charged Pd catalyst complexes were first deposited on oppositely charged functional surfaces, and then were reduced to elemental nickel (0) selectively where the Pd complex was deposited on the surface. In this work, it was demonstrated that selective electroless nickel plating on complex 3-D microstructures with submicron resolution could be achieved using a two-step electroless plating method.

Introduction

Functional and topographical structured surfaces at the micron or nano scale have attracted great attention for their important applications in sensors, optoelectronics, photonics, plastic electronics, and other devices.[1,2] It is therefore practically and fundamentally interesting to create a wide variety of such structured surfaces through the controlled and selective deposition of polymers, colloids, and metals for those potential applications.[3−18] To improve the optoelectronic properties of such patterned and functional surfaces, metal nanoparticle embedded or coated metal−polymer hybrid surfaces are suggested for the fabrication of micro/nano devices and machines.[7,9,10,16,17,19−24] Electroless deposition is a well-known quick, low cost, and low energy process for an alternative metallization technique, and it can become a practical step for the fabrication of optoelectronic devices.[8,10−12,15,16,23−26] Recently, the deposition of metal nanoparticles or quantum dots on colloidal particles, such as silica spheres or polymer beads, has been reported.[27−29] These depositions have potential

* To whom correspondence should be addressed. E-mail: leeil@egr.msu.edu.
† Department of Chemical Engineering.
‡ Department of Materials Science and Engineering.

(1) Arregui, F. J.; Matias, I. R.; Cooper, K. L.; Claus, R. O. *Opt. Lett.* **2001**, *26*, 131−133.
(2) Payne, D. A.; Clem, P. G. *J. Electroceram.* **1999**, *3*, 163−172.
(3) Dai, J.; Bruening, M. L. *Nano Lett.* **2002**, *2*, 497−501.
(4) Decher, G. *Science* **1997**, *277*, 1232−1237.
(5) Hammond, P. T. *Curr. Opin. Colloid Interface Sci.* **2000**, *4*, 430−442.
(6) Joly, S.; Kane, R.; Radzilowski, L.; Wang, T. C.; Wu, A.; Cohen, R. E.; Thomas, E. L.; Rubner, M. F. *Langmuir* **2000**, *16*, 1354−1359.
(7) Brittain, S. T.; Schueller, O. J. A.; Wu, H. K.; Whitesides, S.; Whitesides, G. M. *J. Phys. Chem. B* **2001**, *105*, 347−350.
(8) Carvalho, A.; Geissler, M.; Schmid, H.; Michel, B.; Delamarche, E. *Langmuir* **2002**, *18*, 2406−2412.
(9) Delamarche, E.; Geissler, M.; Bernard, A.; Wolf, H.; Michel, B.; Hilborn, J.; Donzel, C. *Adv. Mater.* **2001**, *13*, 1164.
(10) Delamarche, E.; Vichiconti, J.; Hall, S. A.; Geissler, M.; Graham, W.; Michel, B.; Nunes, R. *Langmuir* **2003**, *19*, 6567−6569.
(11) Delamarche, E.; Geissler, M.; Vichiconti, J.; Graham, W. S.; Andry, P. A.; Flake, J. C.; Fryer, P. M.; Nunes, R. W.; Michel, B.; O'Sullivan, E. J.; Schmid, H.; Wolf, H.; Wisnieff, R. L. *Langmuir* **2003**, *19*, 5923−5935.
(12) Geissler, M.; Kind, H.; Schmidt-Winkel, P.; Michel, B.; Delamarche, E. *Langmuir* **2003**, *19*, 6283−6296.
(13) Guo, T. F.; Chang, S. C.; Pyo, S.; Yang, Y. *Langmuir* **2002**, *18*, 8142−8147.
(14) Kim, E.; Kumar, A.; Whitesides, G. M. *J. Electrochem. Soc.* **1995**, *142*, 628−633.
(15) Kind, H.; Geissler, M.; Schmid, H.; Michel, B.; Kern, K.; Delamarche, E. *Langmuir* **2000**, *16*, 6367−6373.
(16) Ma, D. I.; Shirey, L.; McCarthy, D.; Thompson, A.; Qadri, S. B.; Dressick, W. J.; Chen, M. S.; Calvert, J. M.; Kapur, R.; Brandow, S. L. *Chem. Mater.* **2002**, *14*, 4586−4594.
(17) Whidden, T. K.; Ferry, D. K.; Kozicki, M. N.; Kim, E.; Kumar, A.; Wilbur, J.; Whitesides, G. M. *Nanotechnology* **1996**, *7*, 447−451.
(18) Yang, X. M.; Peters, R. D.; Kim, T. K.; Nealey, P. F.; Brandow, S. L.; Chen, M. S.; Shirey, L. M.; Dressick, W. J. *Langmuir* **2001**, *17*, 228−233.
(19) Brown, K. R.; Natan, M. J. *Langmuir* **1998**, *14*, 726−728.
(20) Murray, C. B.; Norris, D. J.; Bawendi, M. G. *J. Am. Chem. Soc.* **1993**, *115*, 8706−8715.
(21) Marques, A. E.; Dos Santos Filho, S. G.; Anvia, A. R.; Sonnenberg, V.; Martino, J. A. *Phys. Status Solidi A* **2001**, *187*, 75−84.
(22) Wang, T. C.; Rubner, M. F.; Cohen, R. E. *Langmuir* **2002**, *18*, 3370−3375.
(23) Calvert, J. M.; Koloski, T. S.; Dressick, W. J.; Dulcey, C. S.; Peckerar, M. C.; Cerrina, F.; Taylor, J. W.; Suh, D. W.; Wood, O. R.; Macdowell, A. A.; Dsouza, R. *Opt. Eng.* **1993**, *32*, 2437−2445.
(24) Geissler, M.; Wolf, H.; Stutz, R.; Delamarche, E.; Grummt, U. W.; Michel, B.; Bietsch, A. *Langmuir* **2003**, *19*, 6301−6311.
(25) Delamarche, E.; Geissler, M.; Magnuson, R. H.; Schmid, H.; Michel, B. *Langmuir* **2003**, *19*, 5892−5897.
(26) Dressick, W. J.; Kondracki, L. M.; Chen, M. S.; Brandow, S. L.; Matijevic, E.; Calvert, J. M. *Colloids Surf., A: Physicochemical and Engineering Aspects* **1996**, *108*, 101−111.
(27) Tessier, P.; Velev, O. D.; Kalambur, A. T.; Lenhoff, A. M.; Rabolt, J. F.; Kaler, E. W. *Adv. Mater.* **2001**, *13*, 396−400.

10.1021/cm034554n CCC: $25.00
Published on Web 11/05/2003

applications in optoelectronic materials. It is particularly advantageous to direct the deposition of particles, and to selectively plate these particle elements once positioned on the substrate. In taking advantage of the metal-coated particles, the controlled arrays of such particles immobilized on a substrate are even more desirable for a practical purpose in sensors and devices, as they can exhibit optically, electronically, or magnetically functionalized and patterned surfaces. In our previous work,[30−33] the systematic control of polystyrene latex particles on surfaces using patterned polyelectrolyte multilayers was reported; here, using this colloidal array technique, combined with a selective metal deposition technique, 3-D metal-coated polystyrene bead arrays on patterned polyelectrolyte multilayer templates will be discussed.

In the metal-coating of functional polystyrene microspheres, the electroless metal plating technique is preferred for its ability to isotropically coat 3-D objects. This chemistry is based on the chemical reduction of metal ions using a reducing agent.[34] Electroless plating creates a uniform coating of metal on the surface. In this process, the kinetics of the electron transfer should be slow enough to prevent the reduction of the metal ions from occurring in solution. In addition, it is desirable that the surface acts as a catalyst to ensure that reduction of metal ions happens only on the surface. For this reason, a catalyst is first deposited on the surfaces. In this work, two Pd-based catalysts, tetraammoniumpalladium chloride ($[Pd(NH_3)_4]Cl_2$) and sodium tetrachloropalladium ($Na_2[PdCl_4]$) have been chosen for a selective and a nonselective nickel deposition, respectively, on negatively charged PS latex colloidal arrays which are deposited on positively charged polyelectrolyte templates. The catalyst loading step directs metal ion reduction selectively at the target surfaces.

For conventional metal deposition on the surface of colloidal particles in solution, where colloidal particles are well dispersed, a two-step metal plating process is commonly used.[28] Catalyst ions are deposited on the surfaces of colloidal particles from the solution, however, several consecutive centrifugation/redispersion steps are required to get rid of the excess catalyst ions before immersing it into the final metal plating bath.[29,35,36] It is complicated to process metal-plated colloids in solution for these reasons, and even more difficult to process the particles and place them on surfaces for device applications after plating is complete. A much easier approach is the preparation of functional colloidal arrays on surfaces followed by the deposition of metals on the surfaces of the patterned particles secured on the substrate. Recently, we have developed a wide variety of topographically and functionally structured metal-plated surfaces based on polyelectrolyte multilayers with μm- to mm-scale control over surface features and surface functionality.[37,38] We have also developed new techniques that include the formation of point-to-point single and clustered particle arrays on surfaces over large areas.[30] Particle arrays on surfaces offer great potential in optical, electrical, and magnetic sensors and devices, and in photonic and bio-chip applications. In this paper, with the help of a two-step metal plating technique, we will discuss the preparation of these metal particle arrays, and a means of selectively plating different surface components of the arrays.

Experimental Section

A poly(dimethylsiloxane) (PDMS, Dow Corning, Midland, MI) stamp containing various sizes of circle patterns was prepared with a Cr photo mask (Advanced Reproductions, Andover, MA) and a corresponding silicon master (Microsystems Technology Lab, MIT). A microcontact printing (μCP) technique[14] with a PDMS stamp was used to prepare a surface with adhesion-promoting and adhesion-resistant regions of alkane thiols created from 16-mercaptohexadecanoic acid (COOH SAM; Aldrich) and 11-mercaptoundecanonic triethylene glycol (EG SAM; synthesized[39]), respectively, on test-grade silicon wafers (Silicon Sense) coated with a thermally evaporated 10-Å thick chromium film and a 1000-Å gold film. Poly(diallyldimethylammonium chloride) (PDAC, Aldrich, Mw 150 000) and sulfonated polystyrene (SPS, Aldrich, Mw 70 000) were used for patterned layer-by-layer templates. A Carl Zeiss slide stainer equipped with a custom-designed ultrasonic bath (Advanced Sonic Processing) was connected to a computer to perform layer-by-layer assembly. Carboxylated polystyrene latex particles (Polysciences) were used for colloidal adsorption on oppositely charged patterned polyelectrolyte templates.

Samples of colloidal arrays on patterned polyelectrolyte templates were pretreated for 10 s with one of two Pd-based catalysts, $Pd(NH_4)_4Cl_2$ (catalyst 1, Strem Chemicals, Newburyport, MA) and $Na_2[PdCl_4]$ (catalyst 2, Aldrich), each prepared at 5 mM concentration in deionized (DI) water (step 1). The pHs of catalyst 1 and 2 solutions were 6.5 and 2, respectively. After the pretreated samples were washed with DI water followed by N_2 drying, they were dipped into a Ni bath (step 2) for about 10 min. The electroless nickel bath contained nickel sulfate (Ni source, 4 g, Aldrich), sodium citrate (complexant, 2 g, Aldrich), lactic acid (buffer, complexant, 1 g, Aldrich), and dimethylamine borane (DMAB) (reductant, 0.2 g, Aldrich) in 100 mL of DI water. The pH of the Ni bath was adjusted to 6.5 ($\pm$0.1) using ammonium hydroxide. The selective Ni-plated samples were observed using an optical microscope with a mounted digital camera, an X-ray photoelectron microscope (XPS, Kratos Axis Ultra), and an electron microscope (FEI XL30 FEG-ESEM). The EM was fitted with an EDAX thin-window X-ray detector and an EDAX Phoenix X-ray analyzer which were used for the chemical analysis (i.e., Energy Dispersive X-ray Spectroscopy, EDXS) of the selectively nickel-plated surfaces. The XPS survey data were acquired with a pass energy of 160 eV using a monochromatic Al source operating at 150 W, and for the high-resolution data aquisition was equipped with a pass energy of 10 eV. To demonstrate the selective nickel plating of colloidal arrays on polyelectrolyte multilayers, two Pd-based catalysts, $[Pd(NH_3)_4]Cl_2$ (catalyst 1) and $Na_2[PdCl_4]$ (catalyst 2) were employed. The

(28) Dokoutchaev, A.; James, J. T.; Koene, S. C.; Pathak, S.; Prakash, G. K. S.; Thompson, M. E. *Chem. Mater.* **1999**, *11*, 2389−2399.
(29) Caseri, W. *Macromol. Rapid Commun.* **2000**, *21*, 705−722.
(30) Lee, I.; Zheng, H.; Rubner, M. F.; Hammond, P. T. *Adv. Mater.* **2002**, *14*, 572−577.
(31) Chen, K. M.; Jiang, X. P.; Kimerling, L. C.; Hammond, P. T. *Langmuir* **2000**, *16*, 7825−7834.
(32) Zheng, H.; Lee, I.; Rubner, M.; Hammond, P. T. *Adv. Mater.* **2002**, *14*, 569−572.
(33) Zheng, H.; Rubner, M.; Hammond, P. T. *Langmuir* **2002**, *18*, 4505−4510.
(34) Riedel, W., Ed. *Electroless Nickel Plating*; Finishing Publications: Metals Park, OH, 1991.
(35) Kobayashi, Y.; Salgueirino-Maceira, V.; Liz-Marzan, L. M. *Chem. Mater.* **2001**, *13*, 1630−1633.
(36) Garg, A. K.; De Jonghe, L. C. *J. Mater. Sci.* **1993**, *28*, 3427−3432.
(37) Jiang, X. P. C. B.; Choi, J.; Rubner, M. F.; Hammond, P. T. To be submitted for publication. .
(38) Wang, T. C.; Chen, B.; Rubner, M. F.; Cohen, R. E. *Langmuir* **2001**, *17*, 6610−6615.
(39) Pale-Grosdemange, C.; Simon, E. S.; Prime, K. L.; Whitesides, G. M. *J. Am. Chem. Soc.* **1991**, *113*, 12−20.

Scheme 1. Overall Scheme of the Micro-Process to Fabricate Selectively Nickel-Coated Colloidal Particle Arrays on Patterned Polyelectrolyte Multilayers (a), and the Basic Scheme of Selective Nickel Plating on the Negatively Charged Colloidal Particles, and Not on the Positively Charged Polyelectrolyte Surface Using a Positive Pd-complex Ion of $[Pd(NH_3)_4]^{2+}$ (b)

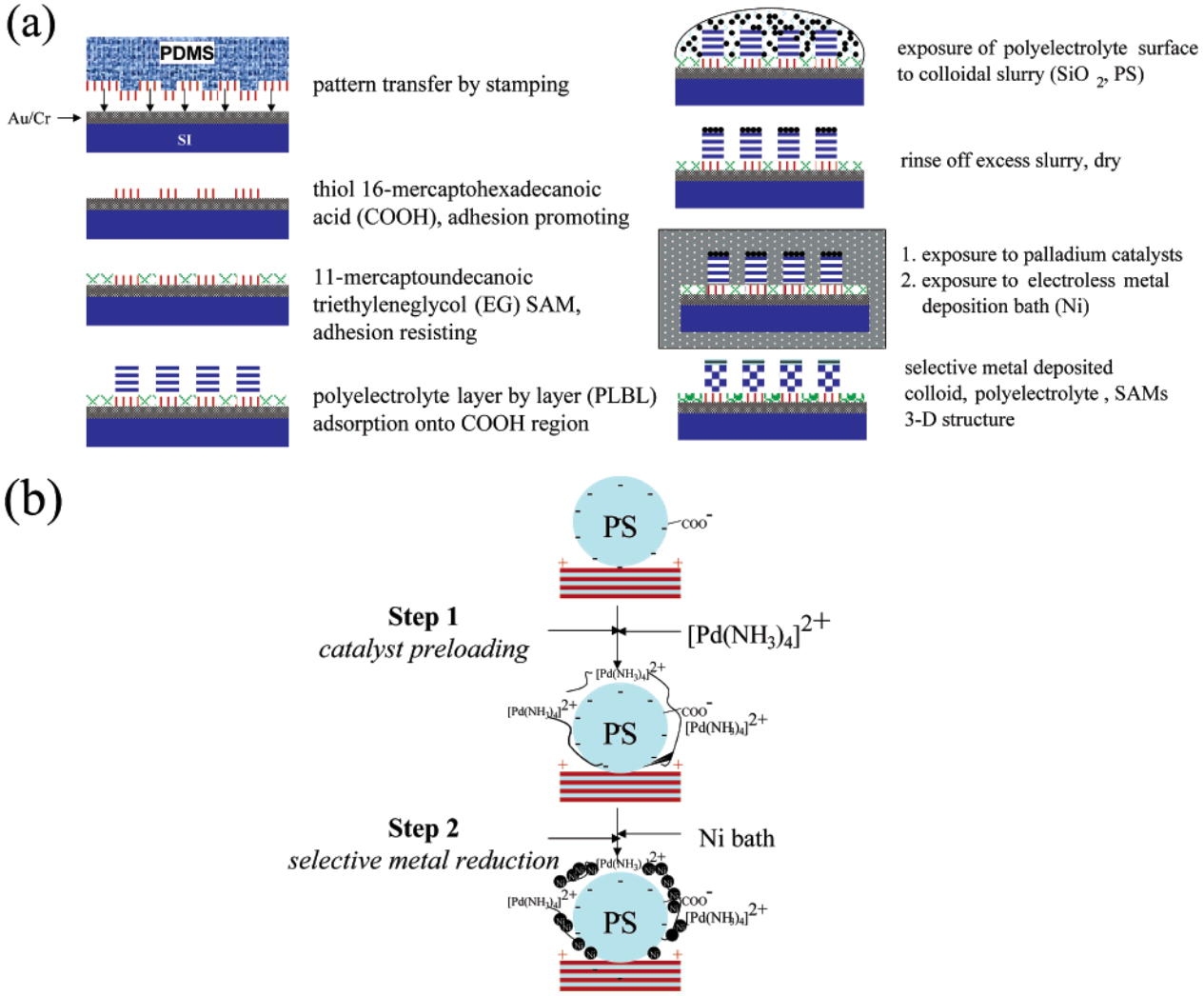

$[Pd(NH_3)_4]Cl_2$ catalyst forms positive Pd-complex ions of $[Pd(NH_3)_4]^{2+}$ that selectively bind to the negatively charged colloid surfaces, directing the redox reaction of Ni^{2+} to Ni to the particle surface. In contrast, no nickel deposition occurs on the positively charged underlying multilayer platforms because of charge repulsion between catalyst 1 and the surface. On the other hand, $Na_2[PdCl_4]$ forms negative complex ions of $[PdCl_4]^{2-}$ and can be used to selectively deposit nickel on positively charged surfaces in solution using the repelling nature of $[PdCl_4]^{2-}$ ions from the same negatively charged surfaces.[38] However, in this work, it was used as a nonselective catalyst, toward the weak electrolytic functional group of −COOH, without pH adjustment in a two-step selective electroless plating process.

Results and Discussion

Scheme 1 shows the overall fabrication scheme of particle arrays via adsorption to patterned multilayer platforms (a), and the selective nickel deposition on the negatively charged colloidal particles, using positive Pd-complex ions of $[Pd(NH_3)_4]^{2+}$ (b). The details of systematic control of the colloidal arrays, even single particle arrays, on the polyelectrolyte multilayers are reported in a previous paper.[30] The selective nickel deposition of the particle arrays on the polyelectrolyte templates are the primary focus and will be discussed in the following three cases: (1) selective nickel deposition of particles randomly deposited on underlying multilayers, (2) selective nickel deposition at the interface between the adhesion-promoting polyelectrolyte template and the adhesion-resisting neutral EG-SAM surface area for charged colloidal deposition, and finally, (3) selective 3-D nickel deposition of particles arrayed on patterned polyelectrolyte multilayers, for which the size of the particles is almost the same as the patterned features of the polyelectrolyte multilayers. To confirm the selective nickel deposition on samples at the micron scale, X-ray photo electron microscopy (XPS) and energy-dispersive X-ray spectroscopy (EDXS) were used, which will be discussed later.

Figure 1 shows the selective nickel-plating of a monolayer of particles randomly adsorbed on polyelectrolyte multilayers, where the oppositely charged colloidal surface (−) and polyelectrolyte surface (+) are the two distinct functional surfaces. Catalyst 1, $Pd(NH_4)_4Cl_2$, (pH ~6.5) was employed in panels a, b, and c, and catalyst 2, $Na_2[PdCl_4]$, (pH ~2) was employed in d. Because of the activity change over time and the difficulty of loading exactly the same amount of the

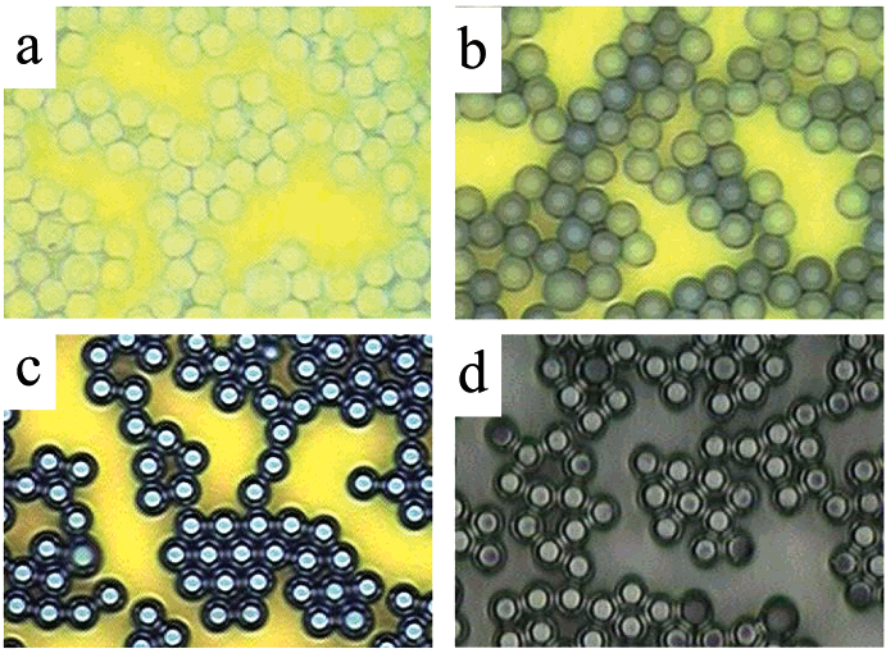

Figure 1. Selective nickel plating on functional polystyrene spheres deposited at random because the carboxylated polystyrene beads are much smaller than the polyelectrolyte multilayer templates. The PS particle is 4.3 μm in diameter and has a negative charge in solution due to the carboxylic acid group. There are 10.5 bilayers of (PDAC/SPS) that are topped with a positively charged layer. The multilayer thickness is 31 nm. In a (few), b (partial), and c (complete), the catalyst 1 ($[Pd(NH_3)_4]Cl_2$) was used in step 1, and in d (nonselective plating), the catalyst 2 ($Na_2[PdCl_4]$) was used instead. The overall deposition kinetics showed some variations depending on the catalyst activity and loading between 5 and 15 min as discussed in the paper, so the same 10-min plating time gave different plating results as shown in a, b, and c.

catalysts, the plating kinetics showed some variation between 5 and 15 min. This resulted in a variation in the extent of plating with a plating time of 10 min in all cases. It must be noted that because of the weak electrolytic nature of particle surface with −COOH group (pK_a ∼4.5),[40,41] the negative particle charge is a variable depending on the solution pH. At a pH lower than pK_a value, the particle surface loses its negative charge, resulting in poor charge repulsion against catalyst 2's complex ion of $[PdCl_4]^{2-}$. Before nickel-plating, the colloidal particles were randomly deposited on oppositely charged homogeneous polyelectrolyte multilayer templates through electrostatic interactions,[30] and remained strongly bound through the entire plating process due to the adhesive nature of the underlying polyelectrolyte multilayers. In the case of using catalyst 1, the nickel ions were preferentially reduced to nickel atoms on the negatively charged colloidal surfaces (a, b, and c), not on the bottom surface of PDAC, which is a strong positive polyelectrolyte independent of pH change (which appears yellow due to the Au substrate). This is due to the affinity of the positive Pd-complex ion, $[Pd(NH_3)_4]^{2+}$, toward the negatively charged colloidal surfaces (step 1), where the pH was higher (6.5) than the pK_a value of −COOH (4.5). Depending on the loaded amount of the $[Pd(NH_3)_4]^{2+}$ ions on the surface of the colloidal particles, and the time in the nickel plating bath, the amount of nickel coated on the colloidal surfaces changed from a transparent layer on the polystyrene bead into an absorbing gray color,and finally to a reflective metallic silver color. The yellow color of the multilayer remained the same, as shown in a, b, and c. In stark contrast, when catalyst 2 was used in the preloading Pd catalyst step, nickel was deposited everywhere, including the colloidal particles and the top PDAC surface of the multilayer film as shown in d. This is explained later with the pH dependency of weak polyelectrolytes having −COOH functional group. In the Pd-complex preloading steps using either catalyst 1 or 2 (step 1), the catalyst preloading time was limited to 10 s, and the nickel-deposition time (step 2) was up to 15 min for both catalyst cases. This suggests that the preloaded Pd catalytic complex on the surfaces played a key role in the selective nickel-plating of the samples during step 2.[38] In the first step of cases a, b, and c, the $[Pd(NH_3)_4]^{2+}$ in solution first deposits on the negatively charged colloidal surfaces and then, during the second step, the Pd-complex aids the nickel ions (+2) to reduce to metallic nickel (0). On the other hand, at a pH of <4.5 the $[PdCl_4]^{2-}$ from catalyst 2 is supposed to bind to the positive PDAC bottom platform instead of the negative colloidal surfaces. However, in this work, using catalyst 2 did not lead to selective nickel plating only on the positive surface, but it led to a nonselective plating that coated both PDAC and the PS particles. This is because the low pH of the catalyst 2 solution (pH ∼2) removed the negative charge of the particle surface by changing $-COO^-$ groups to −COOH at a pH ∼2 in the catalyst loading step, resulting in surfaces that are poorly resistant to the negative Pd complex. At a pH lower than 4.5, the carboxylic acid groups on the colloidal surfaces are not strongly charged enough to fully repel $[PdCl_4]^{2-}$; therefore binding occurs on the particle surfaces during the catalyst loading step. This poor resistance of Pd catalyst complex by the particle surface resulted in the entire nickel plating as shown in Figure 1d. However,

(40) Yoo, D.; Shratori, S. S.; Rubner, M. F. *Macromolecules* **1998**, *31*, 4309−4318.
(41) Sriatori, S. S.; Rubner, M. F. *Macromolecules* **2000**, *33*, 4213−4219.

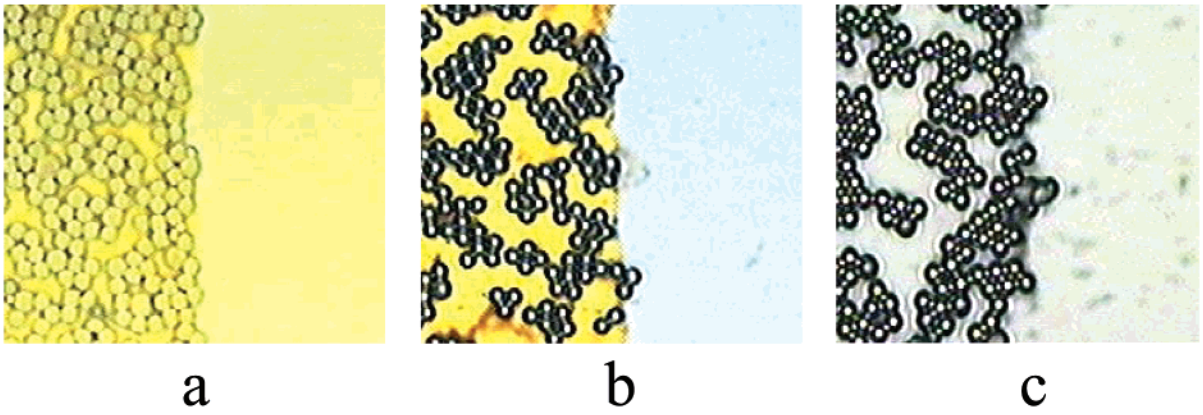

Figure 2. Selective nickel plating at the interface of colloidal adhesion-promoting polyelectrolyte multilayer region (left) and EG-SAM adhesive resisting area (right). Before nickel-plating, negatively charged particles were selectively adsorbed on the positively charged polyelectrolyte multilayer template region (left) (a). In (b) catalyst 1, $[Pd(NH_3)_4]Cl_2$, was preloaded before nickel plating; selective nickel plating was selectively made on the carboxylated polystyene beads ($D = 4.3\ \mu$m) and the EG-SAM area, not on the polyelectrolyte multilayers, $(PDAC/SPS)_{10.5}$. In (c) catalyst 2 ($Na_2[PdCl_4]$) was used to show nonselective nickel plating.

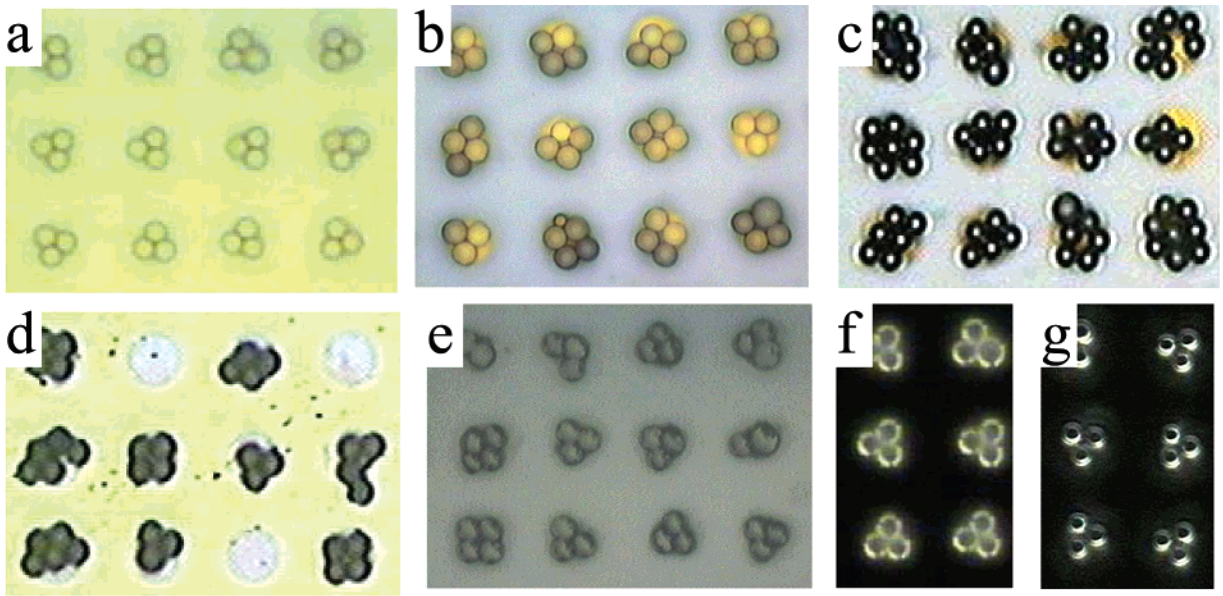

Figure 3. Demonstration of various two-step selective nickel-platings of carboxylated polystyrene bead ($D = 4.3\ \mu$m) arrays deposited on patterned polyelectrolyte multilayer templates, $(PDAC/SPS)_{10.5}$. Catalyst 1 ($[Pd(NH_3)_4]Cl_2$) was used in (b), (c), and (g), and catalyst 2 ($Na_2[PdCl_4]$) was used in (d) and (e). (a) A patterned PS bead array on patterned polyelectrolyte templates before nickel plating. (b) Nickel plating on both the carboxylated PS beads and the EG-SAM area (outside circle) was partially made. (c) Nickel plating was completed, and incomplete particle array shows the uncoated multilayer template (yellow). (d) After several dehydration steps of the EG-SAM area before step 1 (dipping samples into 0.5 M NaOH solution followed by air-drying), the EG-SAM area became inert toward the nickel deposition due to the dehydration of EG functional groups. The incomplete particle array was chosen to show that nickel was also plated on the multilayer platform (blue). (e) Nonselective nickel-plating was made using catalyst 2. (f) Dark-field image of uncoated particle array of sample (a). (g) shows the dark-field image of a nickel coated array which reflects the incident light.

it is expected that there were different kinetics for the nickel depositions on the strong positively charged polyelectrolyte surface (PDAC) and on the weak negatively charged particle surfaces. Actually, a selective nickel plating with catalyst 2 on −COOH surface could be achieved at a pH >4.5, as was demonstrated in the other work.[38] However, in this work, the main focus is the selective nickel deposition on the negatively charged colloidal surface, further work using the catalyst 1 is explored in this paper. When using catalyst 1, all the processes were performed at pH 6.5 (±0.1), where the −COOH groups remained fully charged as $-COO^-$, to attract the positive Pd-complexes.

Figure 2 shows the clear selective nickel-plating of colloidal arrays on the patterned polyelectrolyte templates. First 10.5 bilayers of (PDAC/SPS) multilayers were deposited on the COOH−SAM adhesion-promoting regions (left) in which the top layer is a positive PDAC area, and then the negatively charged carboxylated PS particles were selectively deposited on the multilayers (left), not on the EG-SAM resisting areas (right) (a). When the positive Pd-complex (catalyst 1) was preloaded on the samples (b), it bound on the negative colloidal surfaces and to the EG-SAM area, because EG is effectively a ligand for Me(+) ions, much like crown ethers. This behavior is used in a separate work for

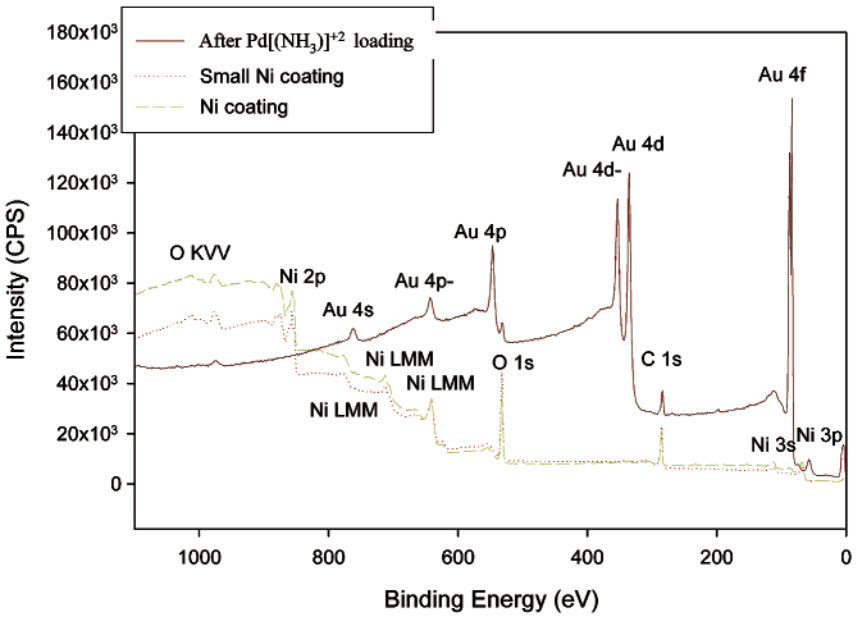

Figure 4. XPS survey scans of samples shown in Figure 3 (a) after $[Pd(NH_3)_4]Cl_2$ loading, Figure 3 (b), and Figure 3 (c).

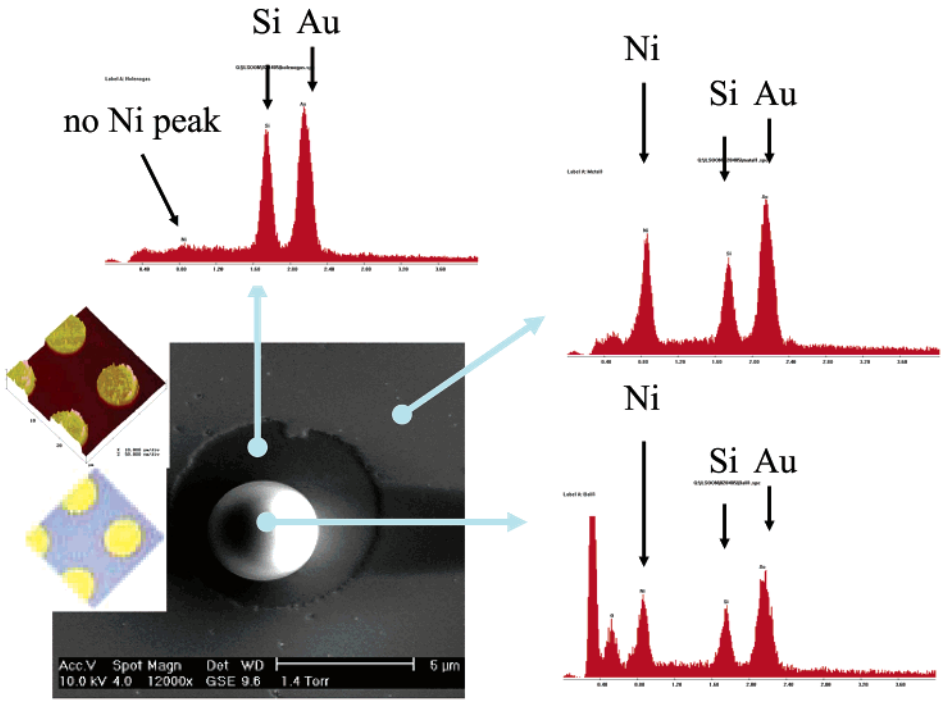

Figure 5. EDXS analysis of selective nickel-plating of samples. Left top and bottom images inserted in the SEM picture are made by an atomic force microscope in a tapping mode (before nickel plating) and by an optical microscope (after nickel plating).

patterned plated lines.[37] Once again, when catalyst 2 was used during the first step, the nickel was deposited everywhere due to the low pH of the catalytic solution (c).

Figure 3 illustrates various cases of the two-step selective nickel-plating results on colloidal arrays. Before the nickel-plating procedure the colloidal particles were adsorbed on patterned polyelectrolyte multilayers (a). As explained above, the negatively charged carboxylated PS latex particles were electrostatically adsorbed on the positively charged patterned polyelectrolyte templates at a pH ~6.5; a detailed micro-processing of the systematic control of the cluster size can be found elsewhere.[30] Regardless of the catalysts used during the preloading step, it was observed that nickel atoms are preferentially reduced on the EG-SAM surfaces. It is believed that the electron lone pairs of the oxygen in EG thiols attract the Pd-complex.[37] Once again, as observed in Figure 1, the amount of nickel coating on the colloidal surface varies with the catalyst loading and the plating time (b and c). On the other hand, when we physically dehydrate the EG-functional groups by treatment with a 0.05 M NaOH solution (several repetitions of dipping samples into a NaOH solution followed by drying),[42] the EG-SAM area remained unplated, retaining its initial green color (d). Instead, the colloidal particles and the PDAC adhesive layers, as shown in

(42) Clark, S. L.; Montague, M. F.; Hammond, P. T. *Macromolecules* **1997**, *30*, 7237−7244.

Table 1. Overall Summary of Selective Nickel Plating on the Model Surfaces at the Micron Scale Using Catalyst 1 and Catalyst 2

model surfaces	catalyst 1	catalyst 2
PDAC	no	yes
PDAC after EG dehydration	no	yes
particle	yes	yes
particle after EG dehydration	no	yes
EG	yes	yes
dehydrated EG	no	no

(d), changed colors. When catalyst 2 was preloaded on the samples, the nickel was deposited everywhere again (e), as in Figure 1(d). The dark-field optical micrograph of (a) is shown in (f). Also, the dark-field optical micrograph of (a) after nickel-plating using catalyst 1 is shown in (g), where the particles are not transparent anymore, and incident light is reflected off the particle surfaces.

Figure 4 shows XPS survey scans of the samples shown in Figure 3(a) after step 1 (using Pd catalyst 1), in Figure 3(b), and in Figure 3(c). After loading catalyst 1, no significant Pd peak was detected, possibly due to the very thin atomic layer of the catalyst which gives rise to a very weak signal compared to the strong Au peaks. However, after short nickel deposition time, the Au peaks almost disappeared due to the thick nickel deposition.

The selective nickel plating was confirmed by EDXS analysis, as shown in Figure 5, where a single particle (adsorbed on a circle featured polyelectrolyte template topped with positively charged PDAC surface), was selectively plated with nickel using catalyst 1. Before Ni plating, the PEM region (inside the circle), was taller than the EG SAM region (outside the circle). After Ni plating, the outside region of the circle feature became higher due to the selective nickel plating on the EG-SAM area. The kinetics of the nickel plating on the EG-SAM area controls the height of the nickel plated area. The kinetics of selective nickel growth on various functional surfaces will be discussed in a separate work.[43] In this work, Figure 5 qualitatively confirms that nickel was selectively plated on the negatively charged particle surfaces and the EG-SAM area, not on the positively charged PDAC template surfaces, which were clearly shown in Figures 2−4 by observation with an optical microscope. The overall findings of the qualitative and selective nickel plating on the model surfaces with submicron resolution are summarized in Table 1.

(43) Lee, I.; Rubner, M.; Hammond, P. T. To be submitted for publication.

Conclusion

Selective electroless nickel deposition on 3-D functional and patterned surfaces was demonstrated at the micron scale with submicron resolution. The microstructure arrays and particle aggregations of carboxylated polystyrene beads on the surface of patterned and homogeneous polyelectrolyte multilayers, respectively, were selectively and nonselectively deposited with nickel by two palladium based catalysts, $[Pd(NH_3)_4]Cl_2$ and $Na_2[PdCl_4]$, using a two-step selective electroless nickel plating technique. Depending on the processing conditions, the Pd-complex ions of the catalysts selectively or nonselectively bind on the target functional groups during the catalyst preloading step, and finally reduce nickel ions to metallic nickel on the target functional surfaces during the second step in a nickel bath. Patterned polyelectroyte multilayers are used as underlying adhesives to immobilize and pattern the colloidal arrays so they will stay on the surfaces during the nickel-plating process. The selective nickel deposition at the micron scale was confirmed by XPS and EDXS analysis. These metallized colloidal surface arrays, due to the nickel deposits, have great potential in many applications in optical, electronic, magnetic, and photonic devices and sensors, as well as in biochips and sensors.

Acknowledgment. We thank Dr. Tom C. Wang and Prof. Robert E. Cohen at the Massachusetts Institute of Technology (MIT) for the discussion on selective nickel-plating, and also Dr. Libby Shaw and Dr. Anthony J. Garratt-Reed at MIT for XPS and EDXS analysis. This work was funded by Hitachi Chemical, Co., Ltd. and made use of MRSEC Shared Facilities supported by the National Science Foundation under Award Number DMR-9400334. We also thank the Center for Fundamental Materials Research at the Michigan State University for funding to finalize this work.

CM034554N